Author Manuscript

Author Manuscript

Author Manuscript

Author Manuscript

HHS Public Access

Author manuscript

Nat Immunol. Author manuscript; available in PMC 2017 March 15.

Published in final edited form as:

Nat Immunol. 2008 October ; 9(10): 1189–1197. doi:10.1038/ni.1654.

Mycobacterium tuberculosis blocks annexin-1 crosslinking and thus apoptotic envelope completion on infected cells to maintain virulence

Huixian Gan[1], **Jinhee Lee**[2], **Fucheng Ren**[2], **Minjian Chen**[1], **Hardy Kornfeld**[2], and **Heinz G. Remold**[1,*]

[1]Brigham & Women's Hospital and Harvard Medical School, Smith Building, Room 526B, 75 Francis Street, Boston, Massachusetts, 02115

[2]Department of Medicine, University of Massachusetts Medical School, Lazare Research Building, 303, 55 Lake Avenue North, Worcester, MA 01655

Abstract

Macrophages infected with attenuated *Mycobacterium tuberculosis* strain H37Ra become apoptotic, limiting bacterial replication and facilitating antigen presentation. Here, we demonstrate that cells infected with H37Ra became apoptotic after formation of an apoptotic envelope on their surface was complete. This process required exposure of phosphatidylserine on the cell surface followed by deposition of the phospholipid-binding protein annexin-1 and then transglutaminase-mediated crosslinking of annexin-1 via its N-terminal domain. In macrophages infected with virulent strain H37Rv, in contrast, the N-terminal domain of annexin-1 was removed by proteolysis thus preventing completion of the apoptotic envelope, which results in macrophage death by necrosis. Host defense of virulent *Mycobacterium tuberculosis* thus occurs by failure to form the apoptotic envelope, which leads to macrophage necrosis and dissemination of infection in the lung.

Introduction

Mycobacterium tuberculosis (*Mtb*), the causative agent of tuberculosis, infects alveolar macrophages which provide a niche for intracellular replication essential to establish host infection [1]. Inhibition of phagosomal acidification and lysosome fusion enable intracellular parasitism by *Mtb* [2]. Apoptosis, a cell death modality that keeps the cell membrane barrier intact, is a common host-defense strategy against intracellular infection. Attenuated *Mtb* complex strains (H37Ra and *Mycobacterium bovis* BCG) induce innate macrophage apoptosis at low multiplicity of infection (MOI) [3, 4]. In contrast, virulent *Mtb* strains suppress that response and instead induce cell lysis and death in a process referred to as necrosis [4-8]. Apoptosis contributes to host-defense from tuberculosis by removing the intracellular macrophage niche by promoting microbicidal activity in macrophages[3, 4, 9] and

Users may view, print, copy, and download text and data-mine the content in such documents, for the purposes of academic research, subject always to the full Conditions of use:http://www.nature.com/authors/editorial_policies/license.html#terms

*Correspondence should be addressed to: H.G.R. (hremold@rics.bwh.harvard.edu).

Author Manuscript Author Manuscript Author Manuscript Author Manuscript

by ‘packaging’ mycobacterial antigens in apoptotic vesicles that enhance presentation by dendritic cells[10, 11]. In contrast, virulent *Mtb* strains activate necrosis, allowing viable bacilli to escape from host cells after which they can infect new cells [12-14].

Although the early events of apoptosis have been extensively studied, the terminal steps required to complete apoptosis have received little attention. Among dying cells, a significant feature of those classified as apoptotic is the presence of an impermeable cell membrane barrier on their outer surface called the apoptotic envelope[15]. With regard to host-defense and responses to apoptotic cells, unique apoptotic envelope surface determinants signal uptake by phagocytes and convey anti-inflammatory signals[16], and the process of apoptosis confines bacilli within membranous vesicles marked for engulfment by recruited phagocytes. In contrast, macrophage necrosis releases viable bacilli for extracellular spread of infection [17] and elicits inflammation contributing to tissue injury and recruitment of naive macrophages that serve as hosts for subsequent rounds of infection. The detrimental impact of macrophage necrosis on tuberculosis defense *in vivo* was demonstrated in studies of the genetic basis for tuberculosis susceptibility in mice[18].

In this study we addressed the mechanism of apoptotic envelope formation in *Mtb*-infected cells, an underappreciated but critical terminal event for *Mtb*-infected macrophages. Formation of the apoptotic envelope involved defined variables including phosphatidylserine ‘flopping’, annexin-1 externalization and crosslinking of annexin-1 by tissue transglutaminase (tTG). Virulent necrosis-inducing *Mtb* strains oppose this process by inducing proteolytic truncation of annexin-1 to a form that cannot be crosslinked. In macrophages infected with attenuated *Mtb* strains, annexin-1 truncation is inhibited by the serine protease inhibitor plasminogen activator inhibitor type 2 (PAI2), which down-regulates the tTG protease activity. Our data support a model to explain the divergent outcomes of *Mtb*-induced macrophage apoptosis or necrosis following infection with virulent or attenuated bacilli *in vitro* and *in vivo*, respectively.

Results

Annexin-1 and PAI2 high molecular weight complexes

We hypothesized that surface exposure of phosphatidylserine (PS) on macrophages undergoing apoptosis after infection with attenuated *Mtb* H37Ra provides binding sites for PS binding proteins that are cross-linked into the developing apoptotic envelope. A search for candidate proteins containing PS-binding and cross-linking domains identified annexin-1, a 37 kDa protein [19, 20] present in abundance on the surface of macrophages infected with attenuated as opposed to virulent *Mtb* [13]. Another candidate for cross-linking is the serine protease inhibitor PAI2, which is produced by many cell types including macrophages [21].

If monomeric 37 kDa annexin-1 is cross-linked into the apoptotic envelope matrix, then it should be present in high molecular weight (MW) protein complexes. Lysates of macrophages undergoing apoptosis after infection with H37Ra contained > 150 kDa annexin-1 complexes detectable by immunoblotting (Fig. 1a, arrow). Of note, uninfected macrophages and other cells [22] frequently show some discrete patches of annexin-1 on the

Author Manuscript Author Manuscript Author Manuscript Author Manuscript

cell surface. In contrast, formation of high molecular weight annexin-1 complexes was significantly diminished in macrophages infected with virulent *Mtb* H37Rv leading to necrosis. These findings established a correlation between high molecular weight annexin-1 and apoptosis.

We next investigated whether high molecular weight annexin-1 complexes accumulate on the surface of H37Ra-infected macrophages taking advantage of the fact that annexin-1 binding to cell membranes is Ca^{++} dependent [19, 23]. EDTA washes of H37Ra-infected macrophages contained two prominent high molecular weight annexin-1 complexes in greater abundance than EDTA washes from uninfected macrophages (Fig. 1b, arrow). Apoptosis therefore correlates with increased formation of a surface matrix containing annexin-1 polymerized into high molecular weight complexes. Immunoblots of the cells after EDTA extraction (Fig. 1b, cells) revealed only the presence of 37 kDa annexin-1, suggesting that annexin-1 polymerization occurs on the cell surface.

To better synchronize the induction of apoptosis for biochemical studies and to evaluate annexin-1 cross-linking in a different context of apoptosis, we treated RAW 264.7 murine macrophages with the apoptosis inducer etoposide [24]. EDTA washes of control and etoposide-treated RAW 264.7 cells were analyzed by immunoblotting for annexin-1 and for PAI2 (Fig. 1c). EDTA extractable material from apoptotic cell surfaces representing < 2 % of total cell protein contained significantly more high M_r annexin-1 complexes than extracts from untreated controls. PAI2 was also present in EDTA washes of apoptotic RAW 264.7 cells in a >175 kDa complex, but was not detectable in washes of untreated cells (Fig. 1c). Lysates of RAW 264.7 cells were immune-precipitated with annexin-1 antibodies and analyzed by immunoblotting with anti-PAI2 (Fig. 1d). A significant amount of PAI2 containing complexes including numerous higher molecular weight complexes, a ~74 kDa component, and the 47 kDa PAI2-monomer were present in anti-annexin-1 precipitates of apoptotic RAW 264.7 cells. Only a small amount of the ~175 kDa molecular PAI2 species were detected in untreated cells. These findings indicated that PAI2 is incorporated into a high molecular weight matrix in apoptotic RAW 264.7 cells. The accumulation of high molecular weight annexin-1 complexes in RAW 264.7 cells was blocked by the tTG inhibitor cystamine (Fig. 1e) [25], which suggests that tTG-mediated protein cross-linking is required for apoptotic envelope formation.

Apoptotic envelope formation requires annexin-1

The preceding experiments showed that annexin-1 is a component of the high molecular weight surface matrix of macrophages undergoing apoptosis after *Mtb* infection or etoposide treatment, but did not clarify whether annexin-1 is a major essential constituent of the apoptotic envelope. Prior studies of synthetic lipid vesicles demonstrated that PS is required for optimal annexin-1 polymerization [26], suggesting that formation of two-dimensionally ordered annexin-1 arrays in planar lipid bilayers facilitates tTG catalyzed cross-linking [27]. We propose that annexin-1 is spatially organized on the surface of apoptotic macrophages by its capacity to bind PS, forming a template required for optimal cross-linking. Consequently, we targeted annexin-1 mRNA by RNA interference (siRNA) in RAW 264.7 cells to test whether reduced annexin-1 production would increase necrosis of etoposide-treated cells

Author Manuscript Author Manuscript Author Manuscript Author Manuscript

(Supplementary Fig. 1a, online). In contrast to vector-treated cells or cells treated with non-targeting siRNA, cells targeted for annexin-1 silencing undergo rapid necrosis after etoposide treatment (Fig. 2a). These data indicated that full-length annexin-1 is essential for the formation of a stable apoptotic envelope, and that an apoptotic cell death mode initiated by etoposide treatment proceeds to necrosis in the absence of annexin-1.

PAI2, which is incorporated into the high molecular weight matrix of apoptotic macrophages, belongs to a group of protease inhibitors that protect cells against injury and mycobacteria induced death[28, 29]. To evaluate a role for PAI2 in apoptotic envelope formation we used the cyclooxygenase (COX) inhibitor indomethacin to inhibit PAI2-synthesis in human macrophages and RAW 264.7 cells [29, 30] (Supplementary Fig. 1b,c online). To exclude unrelated effects of indomethacin we also tested macrophages of PAI2-deficient mice (*Serpinb2*$^{-/-}$). Infection with H37Ra induced apoptosis but little necrosis in untreated human or wild-type murine macrophages. In contrast, H37Ra infection of indomethacin-treated macrophages or of PAI2-deficient murine macrophages resulted in necrosis (Fig. 2b,c and Supplementary Fig. 2). Adding recombinant PAI2 (rPAI2) to PAI2-depleted or PAI2-deficient macrophage cultures prevented necrosis. Exogenous rPAI2 alone had no effect on apoptosis detected by *in situ* TUNEL assay (31 ± 4 % in indomethacin-treated cells infected with H37Ra for 48 h versus 37 ± 4 % in indomethacin and PAI2 treated and infected cells; $n = 3$, $P = 0.36$). Reduced PAI2 production might contribute to necrosis of macrophages infected with virulent *Mtb*, as H37Rv does not induce PAI2 mRNA accumulation whereas this mRNA was highly expressed in H37Ra-infected macrophages (Fig. 2d).

Annexin-1 is cleaved by virulent *Mtb*

The finding that PAI2 protects the completion of apoptosis and prevents necrosis suggests that it inhibits proteolysis of proteins involved in generating the macrophages surface-associated high molecular weight protein matrix. We postulate that 37 kDa annexin-1 is essential for matrix formation because it binds to PS and is a substrate for cross-linking by tTG [26]. The N-terminal annexin-1 domain contains glutamines available for cross-linking at positions 10, 19 and 23 [23]. Proteolytic excision of this domain results in a 34 kDa annexin-1 that cannot be cross-linked [26] yet binds PS on the cell surface more avidly than 37 kDa annexin-1 [23]. We therefore investigated whether PAI2 inhibits annexin-1 proteolysis. Compared to infection with H37Ra, infection of macrophages with virulent H37Rv resulted in significantly increased annexin-1 cleavage to the 34 kDa fragment (Fig. 3a). Depleting endogenous PAI2 with indomethacin increased the amount of cleaved 34 kDa annexin-1 in H37Ra-infected macrophages and this effect was blocked by addition of rPAI2 (Fig. 3b). Proteolysis of the 37 kDa annexin-1 in H37Rv-infected macrophages was inhibited by exogenous rPAI2 (Fig. 3c). These findings suggest that increased proteolytic cleavage of annexin-1 in H37Rv-infected macrophages is a consequence of reduced PAI2 synthesis.

Lipopolysaccharide (LPS) induces PAI2 production by enhancing PAI2 gene transcription and by increasing the half life of the PAI2 transcripts [31]. To test whether LPS induced PAI2 mRNA accumulation is affected by *Mtb* we incubated macrophages with LPS and infected the cells with virulent H37Rv. H37Rv abrogated LPS-induced PAI2 mRNA accumulation

Author Manuscript Author Manuscript Author Manuscript Author Manuscript

(Fig. 4a) suggesting that an active process inhibits this event. In contrast, inoculation with the attenuated H37Ra did not down-regulate LPS-induced PAI2 mRNA accumulation (not shown). High levels of lipoxin A $_4$ (LXA_4), an anti-inflammatory eicosanoid [32], correlate with increased susceptibility to *Mtb* infection [33]. We therefore measured LXA_4 production and found its concentration increased in H37Rv-infected macrophages in contrast to H37Ra infected macrophages suggesting a role for LXA_4 in suppression of PAI2 synthesis (Fig. 4b). Indeed, exogenous LXA_4 significantly inhibited PAI2 expression in H37Ra-infected macrophages (Fig. 4c). These experiments identify LXA_4 produced by H37Rv-infected macrophages as an important down regulator of PAI2 production leading to increased proteolytic cleavage of 37 kDa annexin-1 and necrosis.

Etoposide treatment of RAW 264.7 cells induced PAI2 production in a COX-dependent manner similar to primary human macrophages infected with H37Ra (Supplementary Fig. 1b,c online). Incubation with indomethacin of etoposide-treated RAW 264.7 cells caused necrosis that was reversed by exogenous rPAI2 (Supplementary Fig. 3a online), while rPAI2 did not alter the number of TUNEL-positive cells (36 ± 7 % versus 35 ± 12 %; $n = 5$, $P = 0.9$). Annexin-1 proteolysis was significantly increased in RAW 264.7 cells treated with indomethacin plus etoposide. This correlated with enhanced necrosis (LDH release due to plasma membrane lysis) and was inhibited by addition of rPAI2 (Supplementary Fig. 3b,c, online). These data indicated that annexin-1 cleavage in RAW 264.7 cells correlates with secondary necrosis due to accumulation of a 34 kDa annexin-1 fragment that cannot be cross-linked.

Annexin-1 is cleaved on or close to the macrophage surface

Our previous findings (Fig. 1b) suggested that annexin-1 cleavage occurs at the macrophages surface. To investigate this further, PAI2-depleted RAW 264.7 cells were treated for 24 h with etoposide after addition of full-length recombinant annexin-1 (r-annexin-1). EDTA washes and corresponding cytosolic lysates were analyzed by immunoblot using annexin-1 antibody (Fig. 3d). The EDTA wash of PAI2-depleted cells predominantly contained the 34 kDa annexin-1 fragment. Adding 37 kDa r-annexin-1 increased the level of the 34 kDa annexin-1 fragment only in the EDTA washes and not in the cytosolic fractions. Only 37 kDa annexin-1 was found in the cytosol and its level was similar whether r-annexin-1 was added to the cells or not. These experiments confirm that cleavage of annexin-1 to the 34 kDa fragment occurs on or close to the cell surface.

To further evaluate the association of annexin-1 with the apoptotic envelope we performed fluorescence microscopy and flow cytometry of primary human macrophages and RAW 264.7 cells permeabilized with digitonin for intracellular staining using 37 kDa annexin-1 antibodies, which do not detect the 34 kDa annexin-1 fragment. Full length 37 kDa annexin-1 accumulated on the surface of H37Ra-infected human macrophages and to a smaller extent on untreated macrophages (Fig. 5a, left and center panels) but was not detected on the surface of necrotic macrophages (Fig. 5a, right panel). Apoptosis of etoposide-treated RAW 264.7 cells was also associated with accumulation of 37 kDa annexin-1 on the cell surface (Fig. 5b,c, etop). In contrast, the 37 kDa annexin-1 fragment did not accumulate on the surface of PAI2-depleted RAW 264.7 cells treated with etoposide

Author Manuscript Author Manuscript Author Manuscript Author Manuscript

(Fig. 5b,c, ‘etop + indo’) and was diffusely distributed within the cell. This indicates that in necrotic RAW 264.7 cells 37 kDa annexin-1 is either not transported to the cell surface or is immediately cleaved upon arrival on the cell surface [34].

To investigate whether proteolysis of 37 kDa annexin-1 inhibits its incorporation into the high molecular weight matrix, primary macrophages and RAW 264.7 cells were depleted of PAI2 and either infected with H37Ra or treated with etoposide for 24 h. Immunoblotting for EDTA-extractable annexin-1 demonstrated a significant reduction of high molecular weight annexin-1^{+} complexes in PAI2-depleted, H37Ra-infected macrophages (Fig. 5d). Likewise, PAI2-depleted RAW 264.7 cells treated with etoposide showed little high molecular weight annexin-1 as did untreated controls (Fig. 5e). Reconstitution with rPAI2 restored high molecular weight matrix formation. These data support the hypothesis that cross-linked 37 kDa annexin-1 forms the high molecular weight matrix that is characteristic of the macrophage apoptotic envelope, and that annexin-1 cleavage prevents apoptotic envelope formation.

Anti-mycobacterial PAI2 activity blocks necrosis

Previously it has been shown that necrotic macrophages do not compromise the viability of the bacilli[12, 14]. Since PAI2 appeared to have a role in macrophage apoptosis we investigated whether it promotes anti-mycobacterial activity. Consistent with prior observations, H37Rv replicated over time in infected human macrophages (MOI 10). In presence of etoposide, an inducer of apoptosis [24], intracellular H37Rv replication was not reduced. However when PAI2 was added, etoposide significantly diminished *Mtb* burden (Fig. 6a). To understand the role of different death modalities in the reduction of the H37Rv burden macrophages necrosis or apoptosis was measured. H37Rv induced necrosis in macrophages which was prevented by addition of exogenous rPAI2 in presence of etoposide (Fig. 6b-e). Moreover, apoptosis was also induced in cultures of H37Rv-infected macrophages treated with etoposide alone or with rPAI2 + etoposide (Fig. 6c,e). PAI2 was not involved in the induction of apoptosis, as there is no significant difference in apoptosis of H37Rv + etoposide-treated and H37Rv + etoposide + PAI2-treated macrophage cultures (Fig. 6c,e). The conclusion drawn from these experiments was that PAI2 enables reduction of H37Rv growth by prevention of macrophage necrosis.

The serpin PAI2 possesses a 33 amino acid C–D inter-helical loop containing glutamine residues at positions 83, 84 and 86[35], making it a potential substrate for tTG-mediated cross-linking. Cross-linked PAI2 is found in trophoblast membranes and in the corneal envelope of keratinocytes[15, 21, 36] and we found that PAI2 is part of the surface matrix of apoptotic RAW 264.7 cells (Fig. 1). Native PAI2 protects HeLa cells from TNF-induced death, whereas PAI2 lacking the C–D inter-helical loop is not protective[37]. We therefore investigated whether PAI2 cross-linking is required for formation of the macrophages apoptotic envelope. We compared the capacity of native PAI2, PAI2Δ65-87 (a mutant lacking the C–D inter-helical domain, but able to interact with urokinase-type plasminogen activator), and PAI2Δ380 (a mutant with the P1 reactive center arginine 380 necessary for protease inhibition replaced by alanine) to protect PAI2-depleted RAW 264.7 cells from etoposide-induced necrosis (Supplementary Fig. 4). PAI2Δ380 did not prevent necrosis, indicating that

Author Manuscript Author Manuscript Author Manuscript Author Manuscript

protease inhibition is required for the anti-necrotic activity of PAI2. On the other hand, ablation of the C–D interhelical loop did not alter the capacity of PAI2 to inhibit necrosis, indicating that PAI2 cross-linking is not required for its anti-necrotic activity. These data are corroborated by evidence that other protease inhibitors lacking an inter-helical domain are able to block programmed cell death[38].

Apoptotic envelope inhibition correlates with increased necrosis

To determine how the observed *in vitro* macrophages cytotoxicity difference between H37Ra and H37Rv relates to *in vivo* conditions, BALB/c mice where challenged with 1×10^5 CFU of either *Mtb* strain by tracheal instillation and then bronchoalveolar lavage (BAL) cell populations were compared 9 and 14 days later. At the 9-day time point there were far more necrotic (propidium iodide-positive) macrophages in the mice challenged with H37Rv than with H37Ra (Fig. 7a). This difference persisted at 14 days (data not shown). BAL cell populations were further analyzed by flow cytometry on day 14 post-*Mtb* challenge with staining for CD11b, CD11c, F4/80, and Gr-1. Significant differences in the composition of lung leukocyte populations were observed. Infection with H37Rv dramatically reduced the number of resident alveolar macrophages (defined as $CD11b^{low}CD11c^{high}$) compared with BAL cells from H37Ra-infected and uninfected mice (mean 5,642 versus 63,798 and 109,203, respectively), while the number of $CD11b^{high}CD11c^{high}$ myeloid dendritic cells (mDC) increased only in the H37Rv-infected mice (Fig. 7b). The airways of H37Rv-infected mice were repopulated with a large number of neutrophils (defined as $F4/80^{-}Gr\text{-}1^{+}$), in marked contrast to the H37Ra-infected mice where neutrophils remained a negligible population (Fig. 7c). The presence of many neutrophils in BAL of H37Rv-infected mice in comparison to BAL of control and H37Ra-infected animals was confirmed visually by Giemsa stain (data not shown). These results suggest that the capacity of H37Rv to promote macrophages necrosis through interference with apoptotic envelope formation contributes to disease manifestations unique to virulent bacilli *in vivo*, producing a pro-inflammatory necrotic milieu that dramatically alters pulmonary leukocyte populations.

Discussion

Mycobacertial virulence depends on invasion of lung macrophages and inhibition of phagosome maturation to create a protected intracellular niche for bacterial replication. The capacity of *Mtb* to survive in macrophages, even in face of interferon-γ activation, presents a challenge to host defense analogous to intracellular infection by viruses. One common strategy to deal with this problem is elimination of infected cells by apoptosis[39]. We previously described an innate TNF-mediated macrophages apoptosis pathway triggered by BCG or H37Ra at low MOI[3,4,40] and that mitochondrial membrane destabilization plays also a major role in the induction of macrophages programmed cell death induced by *Mtb* [13].Other innate apoptosis pathways have been described[41, 42], and apoptosis is also a major outcome of the adaptive immune response to infected macrophages through Fas signaling and the actions of granzymes[9,43]. In addition to eliminating the niche for mycobacterial replication, apoptosis creates an intracellular environment hostile to *Mtb*[3-5, 9], and sequesters bacilli in apoptotic bodies that facilitate antigen presentation by dendritic cells[10, 11] as well as engulfment and enhanced killing by newly recruited phagocytes[14, 17].

Author Manuscript Author Manuscript Author Manuscript Author Manuscript

Initial macrophage apoptosis is down-regulated by virulent *Mtb* strains that promote macrophage necrosis, particularly at high intracellular bacillary loads [12, 13]. Necrosis is detrimental to host defense against tuberculosis. It releases viable intracellular bacilli for spreading infection and promotes tissue damage characteristic of advanced tuberculosis disease, a conclusion supported by previous work[18] identifying a tuberculosis susceptibility allele in mice associated with increased necrosis of infected macrophages *in vitro* and giant necrotic lung lesions *in vivo*. The outcome of tuberculosis disease appears to reflect the relative ability of the host to limit *Mtb* growth and spread by containment in apoptotic bodies versus the ability of the pathogen to grow intracellularly and then exit infected macrophages by inducing a death mode with predominant features of necrosis.

The initiation of apoptosis by *Mtb* has generated considerable interest recently, but down stream events culminating in the formation of the apoptotic envelope have not been considered. Here we present the novel finding that macrophages apoptosis induced by attenuated H37Ra leads to formation of apoptotic envelopes by tTG-dependent cross-linking of annexin-1 and PAI2. Infection with virulent H37Rv is associated with annexin-1 cleavage to a form that cannot be cross-linked. This prevents formation of the apoptotic envelope matrix and results in necrosis of the infected macrophages. We confirmed these findings in *Mtb*-infected primary macrophages of human and murine origin and in RAW 264.7 cells and we determined that annexin-1 cross-linking is essential for apoptotic envelope formation in the very different context of etoposide-induced apoptosis. This indicates that our findings represent a general mechanism of apoptotic envelope formation.

We could further show by *in vivo* experiments that lack of apoptotic envelope formation correlates with rampant necrosis. In mice challenged by tracheal instillation of virulent H37Rv significantly more necrotic cells were found in the lungs at day 9 after infection which correlated with a significant depletion of alveolar macrophages and was followed by a dramatic influx of neutrophils[44]. Neutrophil influx is known to occur, when massive necrotic events trigger production of inflammatory chemokines[45].

We propose the following sequence of events leading to apoptotic envelope formation in *Mtb*-infected macrophages. Infection triggers PS exposure on the macrophages surface followed by annexin-1 translocation to the outer plasma membrane leaflet. Binding of annexin-1 to PS on the cell surface[46] arranges it in a two-dimensional array that facilitates cross-linking by tTG to form a stable apoptotic envelope[26]. However, 37 kDa annexin-1 deposited on the cell surface may be cleaved by endogenous proteases to a 34 kDa form that avidly binds PS but cannot be cross-linked by tTG. If cross-linking is not achieved, the apoptotic envelope matrix fails to form and the cell progresses to necrosis. The as yet unidentified endogenous protease(s) involved in that reaction is inhibited by PAI2. Down-regulation of PAI2 (as occurs after H37Rv infection) increases accumulation of 34 kDa annexin-1, prevents apoptotic envelope formation, and promotes cell membrane disintegration and necrosis. The differences between apoptosis and necrosis induced by attenuated and virulent *Mtb* are not likely to be absolute since multiple cell death pathways may be invoked, but our data demonstrate that competition between tTG-dependent cross-linking and proteolytic cleavage of annexin-1 on the macrophages surface may be a physiologically important equilibrium influenced by host and pathogen variables.

Author Manuscript Author Manuscript Author Manuscript Author Manuscript

Studies in other systems corroborate our model. Apoptosis of rat liver cells, human epidermal cells and human lung cancer cells leads to synthesis of a SDS-insoluble polymer formed by tTG-mediated cross-linking of proteins including annexin-1 and PAI2[15,21,47-50]. Recently it was shown that the plasminogen activator Pla, a surface proteinase produced by *Yersinia pestis*, is essential for the development of primary pneumonic plague, a usually lethal necrotizing lung infection, while it is not involved in the development of the bubonic form of plague[51]. In this context it is tempting to speculate that Pla processes annexin-1 into the truncated 34 kDa form leading to massive necrosis and inflammation of the lung tissue.

The Clade B serpin PAI2 inhibits urokinase-type plasminogen activator (uPA) which converts plasminogen to plasmin[52]. Most serpins are intracellular proteins; prior studies of PAI2 were predominantly aimed at identifying an intracellular role due to its inefficient signal sequence[53]. In contrast, our studies indicate that PAI2 acts on the cell surface to prevent annexin-1 proteolysis. PAI2 has a reactive side loop containing the P1-P1′ amino acid residues, that interacts with the active site serine of the target protease [54]. The P1-arginine 380 is required for inhibition of uPA activity and inhibition of cell death in other systems[38]. A second attribute of PAI2 necessary for inhibition of cell death is the 33 amino acid loop between helices C and D, which contains 3 glutamine residues necessary for cross-linking resulting in a co-polymerized but functionally active PAI2 [35-37]. In contrast to the previous findings, we found that PAI2 lacking the 33 residue amino acid loop is as active as native PAI2 for blocking necrosis of macrophages undergoing etoposide-mediated apoptosis. PAI2 lacking the C-D inter-helical loop binds to the active site of uPA, the *bona fide* substrate for PAI2 [55] forming a covalent complex and inactivates uPA as efficiently as native PAI2. Therefore, cross-linking of PAI2 into the apoptotic envelope is not required for protection of annexin-1 from proteolysis under *in vitro* conditions, although it remains possible that tethering the serpin to the nascent apoptotic envelope *in vivo* prevents its diffusion under limiting conditions.

Apoptosis and necrosis are increasingly recognized to exert contrasting influences in tuberculosis defense and pathogenesis. In general terms, necrosis is understood to occur after bioenergetic collapse [56] or as a unique regulated death mode called programmed necrosis [57]. Our data define a new pathway to necrosis caused by the failure of a stable envelope matrix to form in macrophages undergoing apoptosis. While much attention has been paid to the initiation of macrophage apoptosis by *Mtb*, the terminal events leading to the formation of stable apoptotic vesicles have not previously been explored. We present evidence that cross-linking of 37 kDa annexin-1 is an essential step for the creation of apoptotic envelopes in *Mtb*-infected macrophages, and that failure to protect full length annexin-1 from cleavage to its 34 kDa form results in necrosis. The differential regulation of PAI2 expression by H37Ra and H37Rv that we describe may account, at least in part, for the predominantly necrotic death of macrophages infected with the latter. Our results reveal that focusing exclusively on early events in apoptosis, such as nuclear fragmentation, gives an incomplete picture of the death mode of macrophages infected with *Mtb*. Investigating the biochemistry and the functions of the apoptotic envelope will provide a better understanding of the mechanisms by which the host sequesters and kills intracellular pathogens and might reveal new targets for drug development and new insights to vaccine development.

Author Manuscript Author Manuscript Author Manuscript Author Manuscript

Methods

Materials

Goat anti-rabbit IgG FITC conjugate (L42001), polyclonal goat anti-rabbit antibody, purified (L43000) (Zymed); rabbit polyclonal anti-annexin-1 antibody (072-13), rabbit anti-Ac2-26 human serum (H-07213) directed against the N-terminal human annexin-1 peptide (Phoenix Pharmaceuticals, Inc); anti-actin (JLA20) and anti-murine annexin-1 (EH17a) antibodies (Hybridoma Bank, The University of Iowa, Iowa); APC-Alexa Fluor-750 CD11b (M1/70) and PE-F4/80 (BM8) antibodies (eBiosciences), human purified recombinant annexin-1 (Biodesign), rabbit IgG (Upstate); protease inhibitor cocktail (Roche); Hepes and DTT (Invitrogen); propidium iodide, 3-(4,5-dimethylthiazol-2-yl)-2,5-diphenyl tetrazolium bromide (MTT), LPS (Sigma).

Bacteria

Mtb H37Rv, H37Ra and *Mycobacterium smegmatis* (American Type Culture Collection) were grown as described [13] and stored at −80°C. Frozen stocks were thawed, sonicated for 10 s, and then allowed to settle for 10 min. Clumps were dispersed by ten aspirations through a 29-gauge needle (Becton Dickinson).

Quantification of mycobacteria

Adherent macrophages were infected with H37Ra or H37Rv at MOI 2, 5 or 10. After 4 h the cells were washed 5× with HBSS and cultured in IMDM (Invitrogen). Mycobacterial growth was measured after cell lysis with 500 μl 0.2 % (wt/vol) SDS in PBS (neutralized with 500 μL 50% (vol/vol) FCS), serial dilution of 100 μL cell lysates from triplicate cultures and plating on 7H10 agar plates (Remel). Colonies were counted after 21 days. Alternatively 100 μL cell lysates were pooled and inoculated into triplicate Bactec 12B vials (Bactec model 460TB, BD Biosciences).

Cells and culture

Mononuclear cells from buffy coat preparations (Research Blood Component Inc) [13], cultured in IMDM containing 10% human AB serum (Gemini) at 2.0×10^6/ml in 6-well plates for 7 days were challenged with *Mtb*. RAW 264.7 cells (American Type Culture Collection) were cultured in RPMI with 10 % (vol/vol) FCS to 2.0×10^6 cells/ml. To deplete PAI2, 100 μM indomethacin was added to the cells before addition of 5 μM etoposide or of *Mtb*. To reconstitute PAI2 5 μg/ml rPAI2 was added. Mice with deleted PAI2 gene (Dr. Ginsburg, University of Michigan, Ann Arbor, MI; Dougherty et al., 1999) were obtained from Dr. Helene F. Rosenberg, NIAID, Laboratory of Allergic Diseases, Bethesda, MD. WT mice were from Jackson Laboratories. Ninety five percent of the murine spleen macrophages isolated by adherence to plastic dishes were macrophages as determined by non-specific esterase stain and staining with CD11b and F4/80 antibodies.

In vitro assays for apoptosis and necrosis

Apoptosis of macrophages *in vitro* was determined using a fluorescent *in situ* TUNEL assay (In Situ Cell Death Detection Kit; TMR Red; Roche) according to the manufacturer's

Author Manuscript Author Manuscript Author Manuscript Author Manuscript

specifications. To measure necrosis, primary macrophages cultures were treated with PI (10 μg/ml in PBS) for 10 min at room temperature, the cover slips washed twice with PBS and examined with a fluorescence microscope. In some experiments apoptosis and necrosis were measured using the cell death detection ELISA^{PLUS} (Roche Diagnostics) photometric enzyme-immunoassay for the quantitative determination of cytoplasmic (apoptosis) and extracellular (necrosis) histone-associated-DNA-fragments according to the specifications of the manufacturer. RAW 264.7 cell necrosis was determined by measuring the L-lactate/NAD oxyreductase (LDH, EC 1.1.1.27) concentration in cell-free supernatants and lysates using an ELISA (Sigma) according to the specifications of the manufacturer, by assessing the number of remaining cells in culture with MTT (3-[4,5-dimethylthiazol-2-yl]-2,5-diphenyltetrazolium bromide, 0.8 mg/ml, 4 h) [58] at 560 nm using a micro plate spectrophotometer, and by FACS analysis gating 7-AAD^{+}annexin-5^{+} cells with the annexin-V–PE apoptosis detection kit (BD Biosciences Pharmingen).

Lipoxin A_4 (LXA_4) assay

LXA_4 was assayed using an ELISA kit (Oxford Biomedical Research) according to the recommendations of the manufacturer.

Determination and fluorescence imaging of 37 kDa cell surface annexin-1

37kDa annexin-1 was assayed by FACS. Human macrophages and RAW 264.7 cells (10^7 cells) were dislodged from plates with a rubber policeman after fixing (2% paraformaldehyde, 15 min), and washed with PBS containing 1% FBS and 0.1% sodium azide. To every well 100 μl of rabbit polyclonal anti-human annexin-1 or anti-AC2-26 (1μg / ml) (Phoenix Pharmaceuticals) was added (25 ° C, 1 h). After washing twice, goat anti-rabbit FITC antibody (Zymed, 1: 200) was added at room temperature for 45 min, the pellets washed three time and then analyzed by FACS. To determine total cell-associated annexin-1, cells were permeabilized with PBS containing 1 % FBS, 0.2 % saponin, and 0.05 % sodium azide before fixation (4°C, 10 min). For fluorescence microscopy, RAW 264.7 cells were cultured in 35-mm glass-bottom micro well dishes at 1.5×10^6 cells/ well. The cells were then subjected to the experimental conditions, washed, and incubated with anti-AC-26 (5 μg / ml) for 30 min and with fluorescent goat anti-rabbit for 30 min. After washing the cells were examined by fluorescence microscopy.

Immunoblotting

Extracts from 5×10^5 cells in Triton ×100 containing buffer (20 mM Tris [pH7.5],1% (vol/vol) Triton ×100, 1% (vol/vol) glycerol, 137mM NaCl, 2mM EDTA, 25 mM β-glycerophosphate, protease inhibitor cocktail, 4°C, 1h) were centrifuged for 10 min at 4° C, and the supernatant saved. Alternatively, the cells were extracted with 2 mM EDTA in PBS (1μL/well for 5 min at 4 °C). Protein was measured with the Bradford assay. Ten μg of the samples was fractionated on a 12% acryl amide gel and the proteins transferred to a Nylon membrane at 4°C. The membrane was blocked with 5% (wt/vol) milk in 10 mM tris HCl buffer, pH 8.0, 150 mM NaCl and 0.5 % (vol/vol) Tween 20 for 1 h and probed with the respective primary antibodies. After three washes the blots were probed with goat anti-rabbit polyclonal antibody for annexin-1 and goat anti mouse polyclonal antibody for actin, ELC chemifluorescence reagent was added and the blots were exposed to Kodak × film.

Author Manuscript Author Manuscript Author Manuscript Author Manuscript

The human PAI2 probe obtained from the J7 plasmid (ATCC) by digestion with *Xba*I. A 0.9 kb (790-1776) fragment was purified by agarose gel electrophoresis and the RNA was extracted (RNeasy extract total RNA kit, Qiagen). Fifteen micrograms of RNA were fractionated on a 1.2 % (vol/vol) formaldehyde gel and transferred to a Hybond membrane (Amersham HYBOND™-N^+ RPN203). The membrane was dried at 80 ° C for 20 min, soaked in 2 × 0.3 M Na citrate buffer, pH 7.0, containing 0.3 M NaCl for 5 min, and pre-hybridized in 10 ml of Rapid Hybridization solution (Amersham) for 30 min at 65 ° C. The probe was labeled with dCTP P^{32} using a random primer labeling kit (Stratagene) and purified over a G50 column (Pharmacia) to exclude unbound radioactivity. Thereafter 100 μl of 2 mg/ml salmon sperm DNA was added to the probe, the solution boiled for 5 min and 5 × 10^7 c.p.m. of the probe was added to a roller bottle containing the blot and hybridized at 65°C for 2 h. Thereafter the membrane was washed with 2× SSC at 25°C for 15 min and with 0.1× SSC at 65 ° C for 15 min. The membrane was then exposed at −80 ° C over night to Kodak Biomax film.

Real-time PCR

Total RNA was isolated from macrophages using the RNA Easy Kit (Qiagen) and then transcribed into cDNA using the Quantitect Reverse Transcription Kit (Qiagen) according to the manufacturer's recommendation. cDNAs were denatured for 10 min at 95°C. Specific DNA fragments were amplified using a Max3000p Stratagene cycler with steps of 15 s at 95°C, 60 s at 60°C, and 30 s at 72° C for 40 PCR cycles. The oligonucleotide primers used for human actin are AGT CCT GTG GCA TTC ACG AAA CTA (forward) and ACT CCT GCT TGC TGA TCC ACA TCT (reverse) and for PAI2 are TCC TTT CCG TGT AAA CTC GGC TCA (forward) and GAA ATT GGC CCG TCC CTT GTT GAA (reverse). The amount of amplified PAI2 DNA fragments was normalized to actin fragments. Results are expressed as an *n*-fold difference in gene expression.

Silencing of the murine annexin-1 gene

Primers from the murine annexin-1 gene (*Anxa1*; Mouse Gene Bank, NM-010730) were used to design siRNAs (Dharmacon). The sequence 269-288 (TCA TTG ACA TTC TTA CCA A, targeted) and the sequence 321-339 (CCG CGT AGT TAC AGG AGA A, non-targeted) with the loop sequence (TTC AAG AGA) and the *Hpa*1 and *Xho*1 cleavage sites was used to produce two short hairpin RNA-1 primers. Construction of the vectors for silencing RAW 264.7 cells is described in the Supplement.

Cell death and population analysis

BALB/c mice (6 - 8 wk old; Charles River Laboratories, Inc.) were infected with *Mtb* H37Ra or H37Rv at a dose of 10^5 bacteria per mouse by tracheal instillation. Briefly, mice were lightly anesthetized with isoflurane and 50 μl of bacterial solution was pipetted into pharyngeal space while the tongue extended to facilitate inhalation. Mice were sacrificed 9 or 14 d after infection and bronchoalveolar lavage cells were collected by flushing lungs three times with 1.5 ml of PBS containing 0.2% (wt/vol) BSA and 0.2 mM EGTA. To maintain viability of BAL cells, the serum concentration was raised to 10% immediately upon cell recovery. Necrosis measured by staining cells with 25 ug/ml of propidium iodide (Molecular probes) for 15 min, after which 1% (vol/vol) paraformaldehyde was added and

Author Manuscript Author Manuscript Author Manuscript Author Manuscript

cell death was measured using an LSRII flow cytometer and FACSDiva software. For population analysis, BAL cells were stained with anti-CD11b-pacific blue, anti-CD11c-PE, anti-F4/80-allophycocyanin (all antibodies from eBiosciences), and anti-Gr-1-PE-Cy7 (BD Pharmingen). Based on four-color staining, resident alveolar macrophages were defined as $CD11b^{low}CD11c^{high}$, myeloid dendritic cells as $CD11b^{high}CD11c^{high}$, and granulocytes as $Gr\text{-}1^{+}F4/80^{-}$.

Statistics

Results are expressed as mean ± s.e. The data were analyzed by using Microsoft Excel Statistical Software (Jandel) using *t* test for normally distributed data with equal variances. A P value < 0.05 was considered statistically significant.

Supplementary Material

Refer to Web version on PubMed Central for supplementary material.

Acknowledgments

Supported by National Institutes of Health (AI50216 and HL064884). We are grateful to Eileen Remold-O'Donnell and Therese Vallerskog for helpful discussions and to Susanna Remold for help with Fig. S 6.

References

1. Leemans JC, et al. Depletion of alveolar macrophages exerts protective effects in pulmonary tuberculosis in mice. J Immunol. 2001; 166:4604–4611. [PubMed: 11254718]
2. Vergne I, Chua J, Singh SB, Deretic V. Cell biology of mycobacterium tuberculosis phagosome. Annu Rev Cell Dev Biol. 2004; 20:367–394. [PubMed: 15473845]
3. Keane J, et al. Infection by Mycobacterium tuberculosis promotes human alveolar macrophage apoptosis. Infect Immun. 1997; 65:298–304. [PubMed: 8975927]
4. Riendeau CJ, Kornfeld H. THP-1 cell apoptosis in response to Mycobacterial infection. Infect Immun. 2003; 71:254–259. [PubMed: 12496173]
5. Keane J, Remold HG, Kornfeld H. Virulent Mycobacterium tuberculosis strains evade apoptosis of infected alveolar macrophages. J Immunol. 2000; 164:2016–2020. [PubMed: 10657653]
6. Spira A, et al. Apoptosis Genes in Human Alveolar Macrophages Infected with Virulent or Attenuated Mycobacterium tuberculosis: A Pivotal Role for Tumor Necrosis Factor. Am J Respir Cell Mol Biol. 2003; 29:545–551. [PubMed: 12748057]
7. Sly LM, Hingley-Wilson SM, Reiner NE, McMaster WR. Survival of Mycobacterium tuberculosis in host macrophages involves resistance to apoptosis dependent upon induction of antiapoptotic Bcl-2 family member Mcl-1. J Immunol. 2003; 170:430–437. [PubMed: 12496428]
8. Balcewicz-Sablinska MK, Keane J, Kornfeld H, Remold HG. Pathogenic Mycobacterium tuberculosis evades apoptosis of host macrophages by release of TNF-R2, resulting in inactivation of TNF-alpha. J Immunol. 1998; 161:2636–2641. [PubMed: 9725266]
9. Oddo M, et al. Fas ligand-induced apoptosis of infected human alveolar macrophages reduces the viability of intracellular *Mycobacterium tuberculosis*. J Immunol. 1998; 160:5448–5454. [PubMed: 9605147]
10. Schaible UE, et al. Apoptosis facilitates antigen presentation to T lymphocytes through MHC-I and CD1 in tuberculosis. Nat Med. 2003; 9:1039–1046. [PubMed: 12872166]
11. Winau F, et al. Apoptotic Vesicles Crossprime CD8 T Cells and Protect against Tuberculosis. Immunity. 2006; 24:105–117. [PubMed: 16413927]

Author Manuscript Author Manuscript Author Manuscript Author Manuscript

12. Park JS, Tamayo MH, Gonzalez-Juarrero M, Orme IM, Ordway DJ. Virulent clinical isolates of Mycobacterium tuberculosis grow rapidly and induce cellular necrosis but minimal apoptosis in murine macrophages. J Leukoc Biol. 2006; 79:80–86. [PubMed: 16275894]
13. Chen M, Gan H, Remold HG. A mechanism of virulence: virulent Mycobacterium tuberculosis strain H37Rv, but not attenuated H37Ra, causes significant mitochondrial inner membrane disruption in macrophages leading to necrosis. J Immunol. 2006; 176:3707–3716. [PubMed: 16517739]
14. Lee J, Remold HG, Ieong MH, Kornfeld H. Macrophage apoptosis in response to high intracellular burden of Mycobacterium tuberculosis is mediated by a novel caspase-independent pathway. J Immunol. 2006; 176:4267–4274. [PubMed: 16547264]
15. Robinson NA, Lapic S, Welter JF, Eckert RL. S100A11, S100A10, annexin I, desmosomal proteins, small proline-rich proteins, plasminogen activator inhibitor-2, and involucrin are components of the cornified envelope of cultured human epidermal keratinocytes. J Biol Chem. 1997; 272:12035–12046. [PubMed: 9115270]
16. Fadok VA, Bratton DL, Henson PM. Phagocyte receptors for apoptotic cells: recognition, uptake, and consequences. J Clin Invest. 2001; 108:957–962. [PubMed: 11581295]
17. Fratazzi C, Arbeit RD, Carini C, Remold HG. Programmed cell death of Mycobacterium avium serovar 4-infected human macrophages prevents mycobacteria from spreading and induces mycobacterial growth inhibition by freshly added, uninfected macrophages. J Immunol. 1997; 158:4320–4327. [PubMed: 9126994]
18. Pan H, et al. Ipr1 gene mediates innate immunity to tuberculosis. Nature. 2005; 434:767–772. [PubMed: 15815631]
19. Schlaepfer DD, Haigler HT. Characterization of Ca2+-dependent phospholipid binding and phosphorylation of lipocortin I. J Biol Chem. 1987; 262:6931–6937. [PubMed: 2952659]
20. Ando Y, Imamura S, Owada MK, Kakunaga T, Kannagi R. Cross-linking of lipocortin I and enhancement of its Ca2+ sensitivity by tissue transglutaminase. Biochem Biophys Res Commun. 1989; 163:944–951. [PubMed: 2571332]
21. Jensen PJ, Wu Q, Janowitz P, Ando Y, Schechter NM. Plasminogen activator inhibitor type 2: an intracellular keratinocyte differentiation product that is incorporated into the cornified envelope. Exp Cell Res. 1995; 217:65–71. [PubMed: 7867722]
22. Traverso V, Morris JF, Flowers RJ, Buckingham J. Lipocortin 1 (annexin 1) in patches associated with the membrane of a lung adenocarcinoma cell line and in the cell cytoplasm. J Cell Sci. 1998; 111:1405–1418. [PubMed: 9570758]
23. Gerke V, Creutz CE, Moss SE. Annexins: linking Ca2+ signalling to membrane dynamics. Nat Rev Mol Cell Biol. 2005; 6:449–461. [PubMed: 15928709]
24. Kaufmann SH, Earnshaw WC. Induction of apoptosis by cancer chemotherapy. Exp Cell Res. 2000; 256:42–49. [PubMed: 10739650]
25. Siefring GE Jr, Apostol AB, Velasco PT, Lorand L. Enzymatic basis for the Ca2+-induced cross-linking of membrane proteins in intact human erythrocytes. Biochemistry. 1978; 17:2598–2604. [PubMed: 28146]
26. Ando Y, Imamura S, Owada MK, Kannagi R. Calcium-induced intracellular cross-linking of lipocortin I by tissue transglutaminase in A431 cells. Augmentation by membrane phospholipids. J Biol Chem. 1991; 266:1101–1108. [PubMed: 1670773]
27. Oling F, Bergsma-Schutter W, Brisson A. Trimers, dimers of trimers, and trimers of trimers are common building blocks of annexin a5 two-dimensional crystals. J Struct Biol. 2001; 133:55–63. [PubMed: 11356064]
28. Dickinson JL, Bates EJ, Ferrante A, Antalis TM. Plasminogen activator inhibitor type 2 inhibits tumor necrosis factor alpha-induced apoptosis. Evidence for an alternate biological function. J Biol Chem. 1995; 270:27894–27904. [PubMed: 7499264]
29. Gan H, Newman GW, Remold HG. Plasminogen activator inhibitor type 2 prevents programmed cell death of human macrophages infected with Mycobacterium avium, serovar 4. J Immunol. 1995; 155:1304–1315. [PubMed: 7636197]

Author Manuscript Author Manuscript Author Manuscript Author Manuscript

30. Costelloe EO, Stacey KJ, Antalis TM, Hume DA. Regulation of the plasminogen activator inhibitor-2 (PAI-2) gene in murine macrophages. Demonstration of a novel pattern of responsiveness to bacterial endotoxin. J Leukoc Biol. 1999; 66:172–182. [PubMed: 10411006]
31. Schwartz BS, Bradshaw JD. Regulation of Plasminogen activator inhibitor mRNA levels in lipopolysaccharide-stimulated human monocytes. Journ Biol Chem. 1992; 267:7089–7094.
32. Levy BD, Clish CB, Schmidt B, Gronert K, Serhan CN. Lipid mediator class switching during acute inflammation signals in resolution. Nature Immunol. 2001; 2:612–619. [PubMed: 11429545]
33. Bafica A, Scanga CA, Serhan C, Machado F, White S, Sher A, Aliberti J. Host control of *Mycobacterium tuberculosis* is regulated by lipoxygenase-dependent lipoxin production. Journ Clin Invest. 2005; 115:1601–1606.
34. Oliani SM, Paul-Clark MJ, Christian HC, Flower RJ, Perretti M. Neutrophil interaction with inflamed postcapillary venule endothelium alters annexin 1 expression. Am J Pathol. 2001; 158:603–615. [PubMed: 11159197]
35. Jensen PH, et al. A unique interhelical insertion in plasminogen activator inhibitor-2 contains three glutamines, Gln83, Gln84, Gln86, essential for transglutaminase-mediated cross-linking. J Biol Chem. 1994; 269:15394–15398. [PubMed: 7910824]
36. Jensen PH, Lorand L, Ebbesen P, Gliemann J. Type-2 plasminogen-activator inhibitor is a substrate for trophoblast transglutaminase and factor XIIIa. Transglutaminase-catalyzed cross-linking to cellular and extracellular structures. Eur J Biochem. 1993; 214:141–146. [PubMed: 8099547]
37. Dickinson JL, Norris BJ, Jensen PH, Antalis TM. The C-D interhelical domain of the serpin plasminogen activator inhibitor-type 2 is required for protection from TNF-alpha induced apoptosis. Cell Death Differ. 1998; 5:163–171. [PubMed: 10200461]
38. Silverman GA, et al. Human clade B serpins (ov-serpins) belong to a cohort of evolutionarily dispersed intracellular proteinase inhibitor clades that protect cells from promiscuous proteolysis. Cell Mol Life Sci. 2004; 61:301–325. [PubMed: 14770295]
39. Barber GN. Host defense, viruses and apoptosis. Cell Death Differ. 2001; 8:113–126. [PubMed: 11313713]
40. Keane J, Shurtleff B, Kornfeld H. TNF-dependent BALB/c murine macrophage apoptosis following Mycobacterium tuberculosis infection inhibits bacillary growth in an IFN-gamma independent manner. Tuberculosis (Edinb). 2002; 82:55–61. [PubMed: 12356455]
41. Ciaramella A, et al. Induction of apoptosis and release of interleukin-1 beta by cell wall-associated 19-kDa lipoprotein during the course of mycobacterial infection. J Infect Dis. 2004; 190:1167–1176. [PubMed: 15319868]
42. Lopez M, et al. The 19-kDa Mycobacterium tuberculosis protein induces macrophage apoptosis through Toll-like receptor-2. J Immunol. 2003; 170:2409–2416. [PubMed: 12594264]
43. Worku S, Hoft DF. Differential effects of control and antigen-specific T cells on intracellular mycobacterial growth. Infect Immun. 2003; 71:1763–1773. [PubMed: 12654790]
44. Wolf AJ, et al. *Mycobacterium tuberculosis* infects dendritic cells with high frequency and impairs their function in vivo. J Immunol. 2007; 179:2509–2519. [PubMed: 17675513]
45. Li M, et al. An essential role of the NF-κB/Toll like receptor pathways In induction of inflammatory and tissue-repair gene expression by necrotic cells. Journ Immunol. 2001; 166:7128–7138.
46. Arur S, et al. Annexin I is an endogenous ligand that mediates apoptotic cell engulfment. Dev Cell. 2003; 4:587–598. [PubMed: 12689596]
47. Knight RL, Hand D, Piacentini M, Griffin M. Characterization of the transglutaminase-mediated large molecular weight polymer from rat liver; its relationship to apoptosis. Eur J Cell Biol. 1993; 60:210–216. [PubMed: 8096461]
48. Steinert PM, Marekov LN. The proteins elafin, filaggrin, keratin intermediate filaments, loricrin, and small proline-rich proteins 1 and 2 are isodipeptide cross-linked components of the human epidermal cornified cell envelope. J Biol Chem. 1995; 270:17702–17711. [PubMed: 7543090]
49. Levitt ML, Gazdar AF, Oie HK, Schuller H, Thacher SM. Cross-linked envelope-related markers for squamous differentiation in human lung cancer cell lines. Cancer Res. 1990; 50:120–128. [PubMed: 1967140]

Author Manuscript Author Manuscript Author Manuscript Author Manuscript

50. Grenard P, et al. Transglutaminase-mediated cross-linking is involved in the stabilization of extracellular matrix in human liver fibrosis. J Hepatol. 2001; 35:367–375. [PubMed: 11592598]
51. Lathem WW, Price PAV, Miller V, Goldman WE. A plasminogen-activating protease specifically controls the development of primary pneumonic plague. Science. 2007; 315:509–513. [PubMed: 17255510]
52. Kruithof EK, Baker MS, Bunn CL. Biological and clinical aspects of plasminogen activator inhibitor type 2. Blood. 1995; 86:4007–4024. [PubMed: 7492756]
53. von HG, Liljestrom P, Mikus P, Andersson H, Ny T. The efficiency of the uncleaved secretion signal in the plasminogen activator inhibitor type 2 protein can be enhanced by point mutations that increase its hydrophobicity. J Biol Chem. 1991; 266:15240–15243. [PubMed: 1714455]
54. Kruithof EK, Vassalli JD, Schleuning WD, Mattaliano RJ, Bachmann F. Purification and characterization of a plasminogen activator inhibitor from the histiocytic lymphoma cell line U-937. J Biol Chem. 1986; 261:11207–11213. [PubMed: 3090045]
55. Vassalli JD, Dayer JM, Wohlwend A, Belin D. Concomitant secretion of prourokinase and of a plasminogen activator-specific inhibitor by cultured human monocytes-macrophages. J Exp Med. 1984; 159:1653–1668. [PubMed: 6374011]
56. Kroemer G, Dallaporta B, Resche-Rigon M. The mitochondrial death/life regulator in apoptosis and necrosis. Annu Rev Physiol. 1998; 60:619–642. [PubMed: 9558479]
57. Chan FK, et al. A role for tumor necrosis factor receptor-2 and receptor-interacting protein in programmed necrosis and antiviral responses. J Biol Chem. 2003; 278:51613–51621. [PubMed: 14532286]
58. Mosmann T. Rapid colorimetric assay for cellular growth and survival: application to proliferation and cytotoxicity assays. J Immunol Methods. 1983; 65:55–63. [PubMed: 6606682]

Author Manuscript Author Manuscript Author Manuscript Author Manuscript

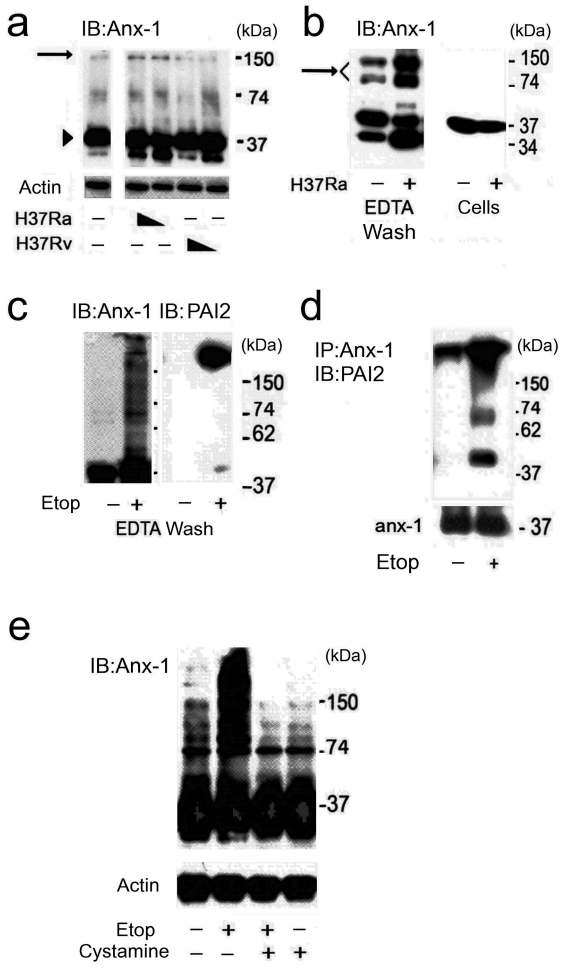

Figure 1. Macrophages undergoing apoptosis form a surface matrix containing cross-linked annexin-1 and PAI2

(**a**) Immunoblot for annexin-1 or actin on lysates of human macrophages infected with *Mtb* strain H37Ra undergoing apoptosis and strain H37Rv undergoing necrosis (MOI 5 and 2) for 48 h. The arrow indicates high molecular weight annexin-1, which is decreased in necrotic macrophages. (**b**) Immunoblot for annexin-1 on lysates of H37Ra-infected (MOI 10) and uninfected macrophages surface-extracted with 2 mM EDTA in PBS. The EDTA wash and the lysed cells were immunoblotted for annexin-1. High molecular weight annexin-1 (arrow). (**c,d**) Immunoassays on RAW 264.7 cells treated with 5 μM etoposide (etop) or control medium for 48 h and then extracted with EDTA and immunoblotted for annexin-1 and PAI2 (**c**) or immunoprecipitated with annexin-1 antibody and immunoblotted for PAI2, or annexin-1 as loading control (**d**). (**e**) Immunoblot for annexin-1 or actin on lysates of RAW 264.7 cells treated with etoposide or control medium in the presence or absence of cystamine. One experiment of three is shown.

Author Manuscript Author Manuscript Author Manuscript Author Manuscript

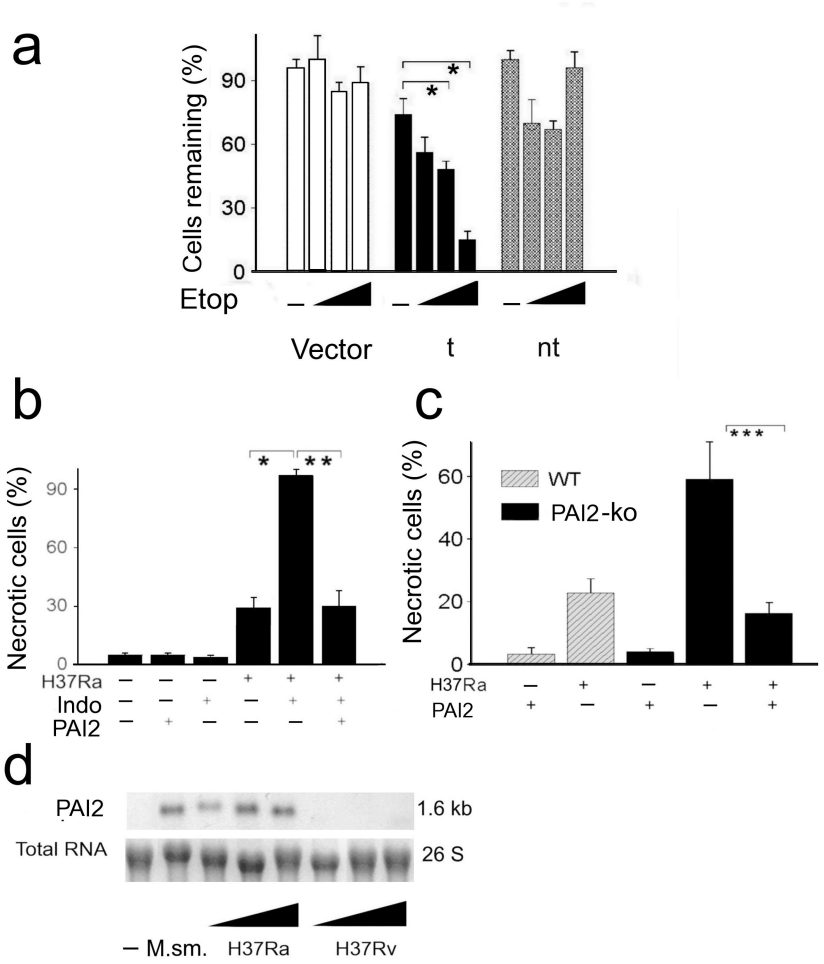

Figure 2. Silencing of annexin-1 abrogates apoptotic envelope formation

(**a**) Spectrophotometry of viable RAW 264.7 cells preincubated with vector alone or annexin-1 targeting or non-targeting siRNA and then treated with 0, 1, 5 and 10 μM etoposide for 48 h. Remaining viable cells were quantified after staining with the vital dye MTT. (**P* = 0.002, *n* = 6).(**b,c**) Fluorescence microscopy for necrotic human macrophages infected with H37Ra (MOI 10, 96h) in the presence or absence of indomethacin and/or rPAI2 (**b**; **P* = 0.07, ** *P* = 0.004, *n* = 4) or murine macrophages from wild-type and PAI2-deficient mice infected with H37Ra (MOI 10, 96 h) without or with rPAI2 (100 μg/ml) (**c;** *** *P* = 0.002, *n* = 3). The cells were stained with PI and counted at magnification ×100. Shown are mean percent PI^+ macrophages ± s.e.(**d**) Immunoblot for PAI2 mRNA and 26S ribosomal RNA expression in human macrophages infected for 24 h with *M. smegmatis* (*M. sm.*), H37Ra or H37Rv (10 h). Shown is a representative from one of four experiments with similar results.

Author Manuscript Author Manuscript Author Manuscript Author Manuscript

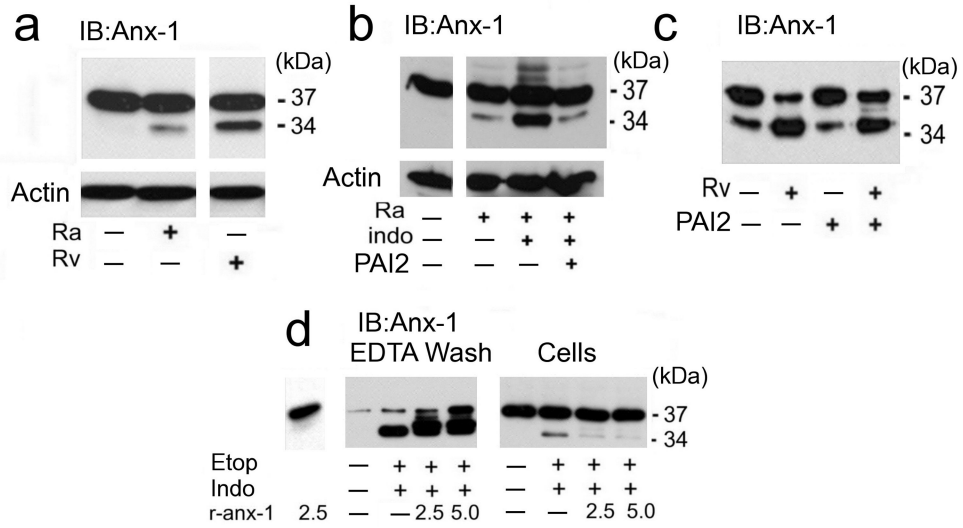

Figure 3. Annexin-1 cleavage is regulated by PAI2

(**a-c**) Immunblots of human macrophages infected with H37Rv (MOI 10, 48 h) (**a,c**) or H37Ra (**a,b**) without (**a**) or with (**b,c**) indomethacin (50 μg/ml) and/or rPAI2 (100 μg/ml), as indicated. Cell lysates were immunoblotted for annexin-1 or actin (**a-c**). (**d**) Immunoblot for annexin-1 of RAW 264.7 cells treated with etoposide (etop), indomethacin, and/or recombinant or annexin-1 (r-anx1; 2.5 or 5 μg/ml), as indicated. The cells were extracted with EDTA and the EDTA washes and cells extracts were immunoblotted. Actin staining verified equal loading (not shown). One of three experiments is shown.

Author Manuscript Author Manuscript Author Manuscript Author Manuscript

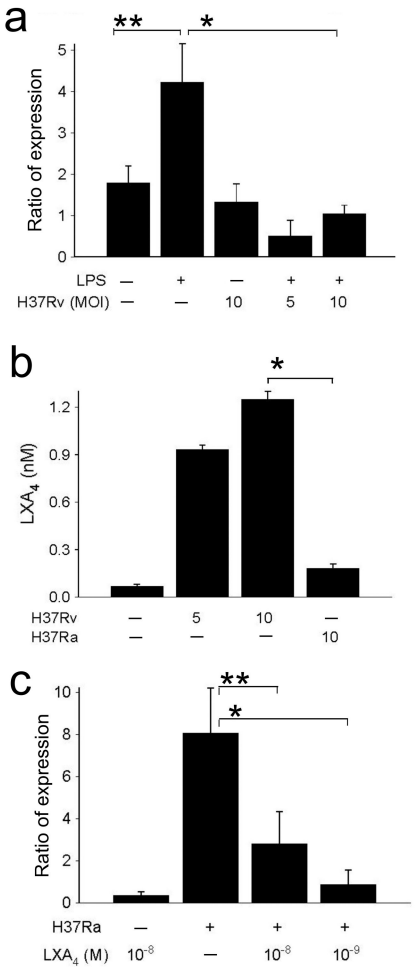

Figure 4. Effect of virulent H37Rv on PAI2 mRNA accumulation

(**a**) RT-PCR for PAI2 and actin mRNAs in macrophages (5×10^5 / plate) cultured with or without LPS (10 ng/ml) and infected at the MOI 10 for 24 h with virulent H37Rv. Ratio of expression refers to the *n*-fold-difference in PAI2 mRNA concentrations normalized to actin mRNA. (**P* = 0.05, ** *P* = 0.01, *n* = 4). (**b**) Virulent H37Rv in contrast to avirulent H37Ra induce production of significant amounts of LXA_4. Macrophages were cultured with H37Ra or H37Rv at the MOI indicated and LXA_4 was measured in the supernatants after 12 h. (**P* = 0.001, *n* = 3). (**c**) RT-PCR for PAI2 and actin mRNAs in macrophages infected with or without H37Ra (MOI 10, 24 h) in presence and absence of LXA_4 at the concentrations indicated. Ratio of expression refers to the *n*-fold-difference in PAI2 mRNA concentrations normalized to actin mRNA (**P* = 0.001, ** *P* = 0.03, *n* = 3).

Author Manuscript Author Manuscript Author Manuscript Author Manuscript

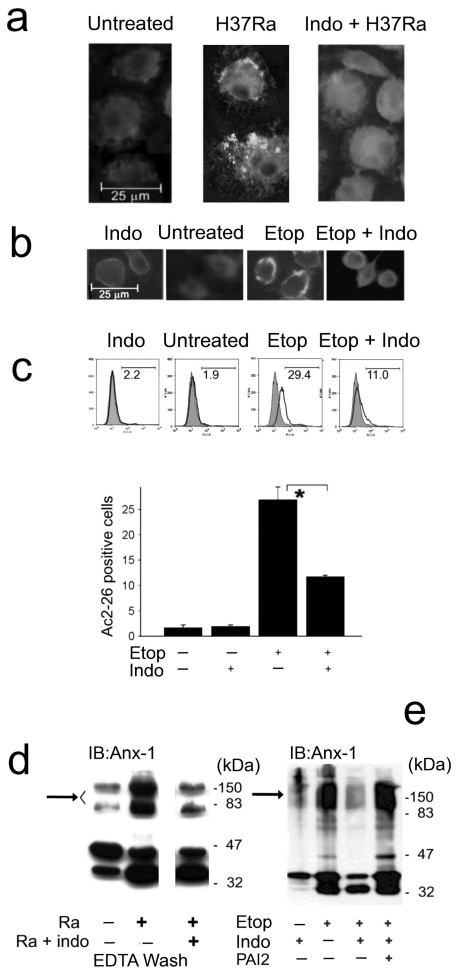

Figure 5. Induction of apoptosis causes annexin-1 accumulation on the macrophage

(**a,b**) Fluorescence microscropy of human macrophages infected with H37Ra (MOI 10, 48 h) in the presence or absence of indomethacin (**a**) and RAW 264.7 cells treated with etoposide for 24 h in the presence or absence of indomethacin (**b**); the cells were permeabilized with digitonin and analyzed after staining with antibody to the N-terminal domain (Ac2-26) of annexin-1. One of three experiments is shown. (**c**) Surface expression of Ac2-26 analyzed by flow cytometry. RAW 264.7 cells treated as in **b** were fixed, surface-stained with Ac2-26 antibody and analyzed. Shown are histograms from a single of three experiments (top) and mean percent Ac2-26-positve cells ± s.e.(bottom, * $P = 0.02$, $n = 3$). (**d,e**) Immunoblots of human macrophages infected with H37Ra in the presence or absence of indomethacin and then EDTA washes of the cells were evaluated for the presence of annexin-1 (**d**) and RAW 264.7 cells treated as indicated with etoposide, and indomethacin and then whole cell lysates were immunoblotted for annexin-1 (**e**). The sample for each condition comes from 10^4 cells. Representative experiments of three are shown.

Author Manuscript Author Manuscript Author Manuscript Author Manuscript

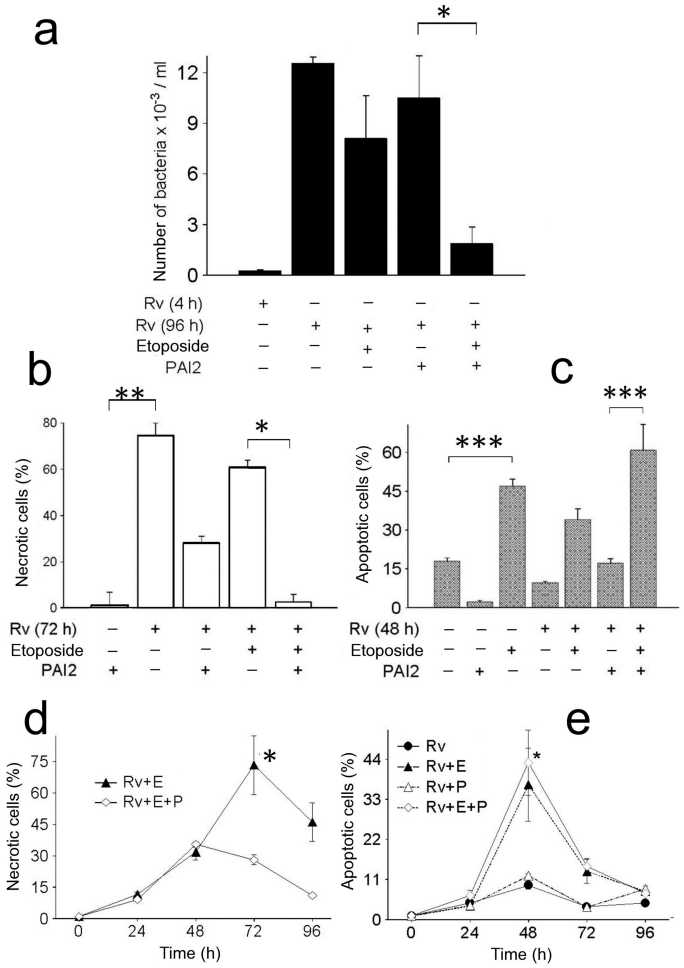

Figure 6. PAI2 protects against macrophages necrosis and contributes to expression of anti-mycobacterial activity in human macrophages infected with H37Rv

(**a-e**) Macrophages infected with H37Rv for the given times and with the reagents indicated. (**a**) Bacterial burden measured at 96 h (**a**, * $P = 0.001$, $n = 6$); (**b**) Flow cytometry for necrotic cells at 72 h as measured by PI+ cells (**b**, at 72 h, ** $P = 0.0001$, $n = 5$; MOI 10; * $P < 0.007$, n - 5); (**c**) TUNEL staining for apoptosis at 48 h (**c**,*** $P = 0.015$, $n = 5$); (**d,e**) ELISA photometric enzyme-immunoassay for necrosis (**d**) and apoptosis (**e**) over the same time course. (**d**, at 72 and 96 h, * $P = 0.001$, $n = 3$; **e**, $P = 0.003$, n = 3). One of three experiments is shown.

Author Manuscript Author Manuscript Author Manuscript Author Manuscript

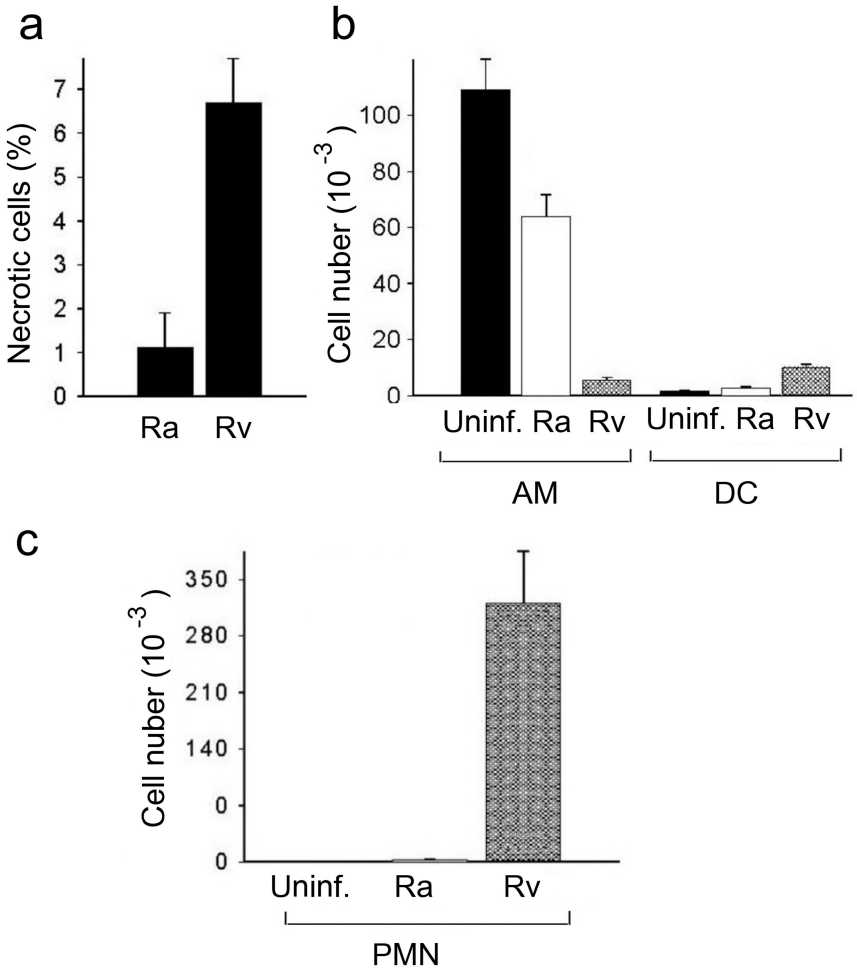

Figure 7. ***In vivo*** **cytotoxicity of virulent** ***Mtb***

(**a-c**) Mice were challenged by tracheal instillation with 10^5 CFU of H37Ra or H37Rv and then cells were recovered for analysis by bronchoalveolar lavage (BAL) 9 or 14 days later. One of three experiments is shown. (**a**) Necrosis of BAL cells 9 days post-infection assessed by PI staining; results are expressed as the mean % PI-positive cells ± s.e.m. ($P = 0.004$, $n = 4$). (**b**) Resident AM and lung mDC defined as $CD11b^{low}CD11c^{high}$ and $CD11b^{high}CD11c^{high}$ cells, respectively, quantified by flow cytometry and hemocytometer counts of total BAL cells on day 14 post-infection; the total number of either cell type in mice infected with H37Ra or H37Rv, or uninfected mice, is expressed as the mean ± s.e.m. ($n = 3$; infection-depleted resident AM, H37Rv versus H37Ra, $P < 0.01$ for differences between all three groups; the number of mDC in the lungs H37Rv versus H37Ra, $P < 0.001$ for Rv vs. control and H37Rv vs. H37Ra). (**c**) Lung neutrophils ($CD11b^{+}Gr\text{-}1^{+}F4/80^{-}$ cells) quantified by flow cytometry and hemocytometer counts of total BAL cells on day 14 post-infection expressed as the mean ± s.e.m. ($n = 3$; $P < 0.001$).